Optical Materials 31 (2008) 440–444

Contents lists available at ScienceDirect

Optical Materials

journal homepage: www.elsevier.com/locate/optmat

Luminescent nanoparticles of $MgAl_2O_4$:Eu,Dy prepared by citrate sol–gel method

Alessandra S. Maia [a], Roberval Stefani [a], Cláudia A. Kodaira [b], Maria C.F.C. Felinto [b], Ercules E.S. Teotonio [c], Hermi F. Brito [a,*]

[a] Instituto de Química, Universidade de São Paulo, C.P. 26077, CEP 05513-970, São Paulo – SP, Brazil
[b] Instituto de Pesquisas Energéticas e Nucleares, Av. Prof. Lineu Prestes 2242, CEP 05508-900, São Paulo – SP, Brazil
[c] Departamento de Química, Universidade Federal de Goiás-Campus Catalão, C.P. 56, CEP 75704-020, Catalão – GO, Brazil

ARTICLE INFO

Article history:
Received 13 June 2007
Received in revised form 9 April 2008
Accepted 19 June 2008
Available online 10 August 2008

Keywords:
Persistent luminescence
Magnesium aluminate
Divalent europium
Trivalent dysprosium
Citrate precursor
Sol–gel method

ABSTRACT

$MgAl_2O_4$:Eu,Dy nanoparticles were prepared by citrate sol–gel method and thermally treated at 600, 700, 800 and 900 °C. The trivalent europium ion is partially reduced to the divalent state at 700 and 800 °C. Infrared spectra of the phosphors showed bands around 700 and 520 cm^{-1} corresponding to the AlO_6 groups. X-ray diffraction patterns present sharp reflections of samples heated from 700 to 900 °C indicating the $MgAl_2O_4$ spinel phase. Grain size in the range 20–30 nm were observed by measurement of transmission electron microscopy (TEM). The emission spectra of the phosphors show a broadened band at 480 nm assigned to the $4f^65d \rightarrow 4f^7$ ($^8S_{7/2}$) transition of Eu^{2+} ion overlapped to the $^4F_{9/2} \rightarrow {}^6H_{15/2}$ transition of the Dy^{3+} ion. Besides, the $^4F_{9/2} \rightarrow {}^6H_{13/2}$ transition (579 nm) of Dy^{3+} ion is overlapped with the $^5D_0 \rightarrow {}^7F_0$ (578 nm) and $^5D_0 \rightarrow {}^7F_1$ (595 nm) transitions from the Eu^{3+} ion. Excitation spectra of the sample heated at 900 °C monitoring the excitation at 615 nm of $^5D_0 \rightarrow {}^7F_2$ transition of Eu^{3+} ion exhibit a broad band assigned to the $O \rightarrow Eu^{3+}$ ligand-to-metal charge-transfer states (LMCT) around 280 nm. The samples present green persistent luminescence after exposure to UV radiation. The chromaticity coordinates were obtained from the luminescence emission spectrum.

1. Introduction

Persistent luminescent materials are part of everyday life, finding large use in applications such as luminous paints, emergency lighting, safe traffic, wall painting, films, artificial fibres, rubbers, textiles ceramics, etc. Divalent europium doped alkaline earth aluminates have attracted interest in this field due to their long persistent luminescence at the blue-green visible region [1,2]. This property has not been well characterized yet, once it deals with very complicated mechanisms and involves lattice defects (vacancies, colour centers) as well as the possibility to have both correlated and uncorrelated centers [3].

The effect of the trivalent rare earth ions RE^{3+} (such as Nd^{3+} or Dy^{3+}) as co-dopant in the oxygen vacancies should also be considered. If an electron is transferred from the trap (i.e., an oxygen vacancy close to the RE^{3+} ion) to the RE^{3+} ion, the RE^{2+} ion (or RE^{3+}-e-entity) could be formed [4]. In this case, the phosphors MAl_2O_4:Eu^{2+},RE^{3+} (M = Ca^{2+} and Sr^{2+}) present excellent luminescent properties like high brightness, long-lasting phosphorescence, high quantum efficiency and great chemical stability. In addition, these materials have another advantage over the traditional sulphide-based phosphors as they lack radioactive elements [5–7].

Solid-state reactions have been widely used to obtain MAl_2O_4:Eu^{2+},Dy^{3+} (M = Ca^{2+} and Sr^{2+}). However, long reaction time (4–10 h) and high temperatures (1300–1500 °C) were required [8,9]. Reducing atmosphere during heat treatments is also necessary to reduce trivalent europium to the divalent state. Besides, the phosphors synthesized by the solid-state routes generally present large grain size. Nevertheless, luminescent properties are greatly dependent on the grain size, leading to attractive properties when the grain size decreases [10]. Therefore, sol–gel routes are efficient alternatives as they offer better purity and homogeneity, and can yield stoichiometric powders with smaller grain size particles at relatively lower processing temperature in comparison with conventional solid-state reaction [11–13].

In this work, the photoluminescent properties of a magnesium aluminate spinel based phosphor, $MgAl_2O_4$:Eu,Dy, prepared by citrate sol–gel method were investigated, since the preparation of persistent luminescent solids in softer conditions are desirable.

2. Experimental

The starting materials used in this work were Merck analytical reagent grade magnesium nitrate, aluminum nitrate, citric acid and ammonium hydroxide. Hydrated europium nitrate and dysprosium nitrate were prepared from the oxides RE_2O_3 (RE = Eu^{3+} and Dy^{3+}) purchased from Aldrich (99.9%). The citrate sol–gel route

* Corresponding author. Tel.: +55 11 3091 3708; fax: +55 11 3815 5579.
E-mail address: hefbrito@iq.usp.br (H.F. Brito).

0925-3467/$ - see front matter © 2008 Elsevier B.V. All rights reserved.
doi:10.1016/j.optmat.2008.06.017

used here was based on the method described by Jia et al. to prepare $MgAl_2O_4$ spinel [14]. An aqueous solution of magnesium nitrate and aluminum nitrate in the molar ratio Mg/Al = 2.05, europium nitrate and dysprosium nitrate in the molar ratio of Eu/Mg = 1% and Dy/Mg = 2% was prepared. To this solution, citric acid aqueous solution in the molar ratio of $H_3Cit/(Mg^{2+} + Al^{3+}) = 1$ was added, then ammonia added, drop by drop up to pH = 5. The final solution was then evaporated slowly in a water bath to form a viscous colloidal gel. The gel was heated at 120 and 240 °C for 3 h in a muffle to form a black porous material. This precursor was finally calcined, in a crucible covered with a lid, at different temperatures (600, 700, 800 and 900 °C) for 5 h in air.

X-ray diffraction (XRD) patterns of the samples were recorded on a Rigaku Miniflex diffractometer using Cu Kα radiation (30 kV and 15 mA) from 2 to 90° and pass time of 1 s. Infrared (IR) spectra of KBr pellets of samples were registered on a BOMEM MB 102 spectrometer.

Photoluminescence measurements were performed in a spectrofluorimeter SPEX-Fluorolog 2 with double grating 0.22 m monochromators (SPEX 1680), and a 450 W Xenon lamp as excitation source. The excitation and emission spectra of the samples were recorded at room and liquid nitrogen temperatures and collected at an angle of 22.5° (front face). All spectra were recorded using a detector mode correction.

The luminescence decay curves of the emitting levels and the time resolved spectra were measured using a phosphorimeter SPEX 1934D accessory coupled to the spectrofluorometer.

Transmission electron microscopy (TEM) images were registered on a LEO 906E microscope operating at 80 kV. Samples were prepared by dispersing the fine powder with ethanol addition, followed by ultrasonic agitation and depositing a droplet of suspension on a copper microscope grid covered with porous carbon film.

The chromaticity coordinates were obtained according to the Commission Internationale de l'Eclairage (CIE) using a Spectra Lux Software v.2.0 Beta [15].

3. Results and discussion

XRD patterns of samples calcined at 600, 700, 800 and 900 °C for 5 h, in air, are shown in Fig. 1. As it can be seen, there is no diffraction peak for the sample heated at 600 °C suggesting an essentially amorphous character. On the other hand, sharp reflections are observed in patterns of samples heated at 700 °C and above, indicating almost complete crystallization in the $MgAl_2O_4$ spinel phase. There is no evidence of any other aluminum or magnesium phases, indicating that the doping with europium (1% mol) and dysprosium (2% mol) ions has nearly no effect on the spinel phase formation [16]. The XRD results were compared with data from the JCPDS card No 21-1152.

IR spectra of samples heated at different temperatures are shown in Fig. 2. In sample heated at 600 °C, bands in the region of 1640–1410 cm^{-1} assigned to carboxylate groups are observed, indicating the high content of carbonaceous material. The intensities of these bands decrease as the temperature of precursor preparation increases. It is also observed that the bands around 700 and 520 cm^{-1}, which correspond to the AlO_6 groups building up the magnesium aluminate spinel, display increased intensities with rising temperature [17].

Transmission electron microscopy (TEM) was performed to determine particle morphology, crystallite size, as well as homogeneity at nanometer scale. TEM images of $MgAl_2O_4$:Eu, Dy sample prepared at 800 °C by citrate sol–gel method are shown in Fig. 3. It revealed aggregates of nanoparticles in sphere-like form with

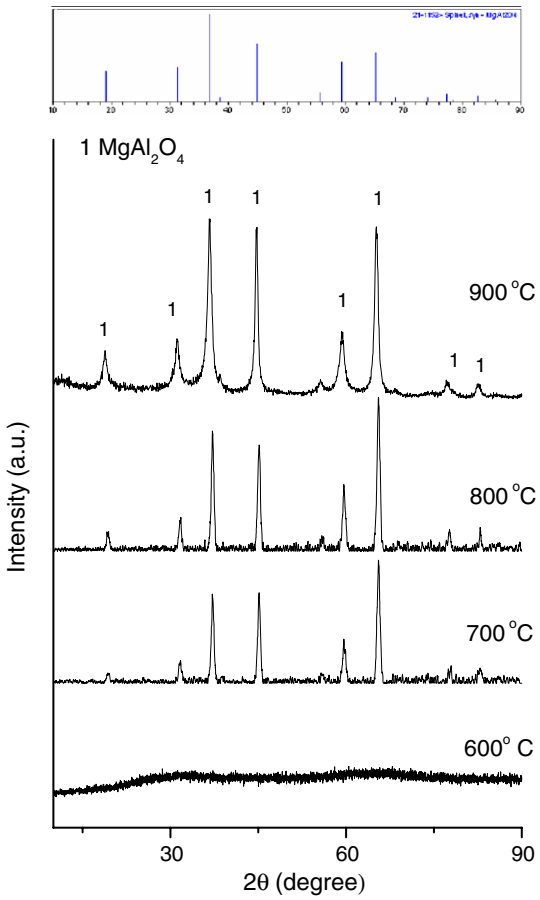

Fig. 1. XRD patterns of $MgAl_2O_4$:Eu, Dy samples heated at different temperatures for 5 h.

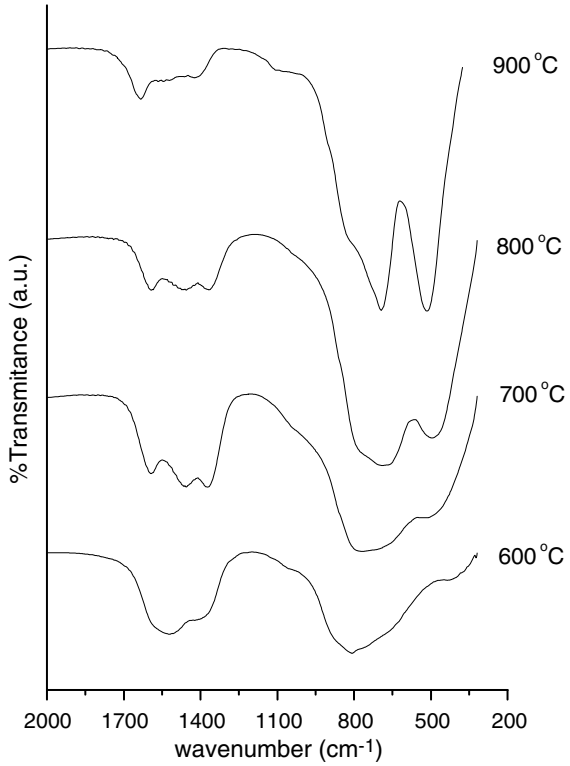

Fig. 2. IR spectra of $MgAl_2O_4$:Eu, Dy samples heated at different temperatures for 5 h.

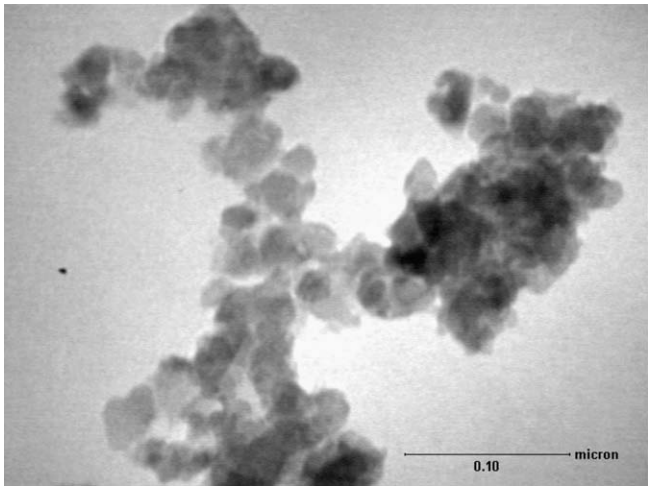

Fig. 3. TEM image of $MgAl_2O_4$:Eu,Dy sample heated at 800 °C for 5 h, with scale 0.10 μm.

grain sizes *ca* 20 nm. Average crystallite sizes determined by Scherrer's equation [16] were 28, 27 and 19 nm for the samples annealing at 700, 800 and 900 °C, respectively. These results show that values of average particle sizes of $MgAl_2O_4$:Eu,Dy system determined by Scherrer's equation are consistent with that obtained by TEM technique (Fig. 3).

$MgAl_2O_4$:Eu,Dy sample heated at 600 °C presents no luminescence under UV-lamp excitation (figure not shown). On the other hand, the samples heated at 700 to 900 °C present green persistent luminescence for some seconds, after interrupting long wavelength UV-lamp (λ_{ex} = 366 nm).

Nowadays, there are several inorganic materials that exhibit persistent luminescence in literature; however, the mechanisms to elucidate this phenomenon are often ambiguous [1,3,18]. Recently, Holsä et al. [4] reported a new persistent luminescence mechanism for the $CaAl_2O_4$:Eu^{2+},RE^{3+} system, based on the photoionization of the electrons from Eu^{2+} to the conduction band followed by the electron trapping to an oxygen vacancy, which is aggregated with a Ca^{2+} vacancy and a RE^{3+} ion.

Excitation spectra of $MgAl_2O_4$:Eu,Dy materials prepared at 700, 800 and 900 °C (Fig. 4) were recorded under emission monitored at 480 nm assigned to the $^4F_{9/2} \rightarrow {}^6H_{13/2}$ intraconfigurational transition of the Dy^{3+} ion overlapped with $4f^65d \rightarrow 4f^7$ ($^8S_{7/2}$) interconfigurational transition of Eu^{2+} ion. These spectra display a broad band with maximum around 340 nm that corresponds to the $4f^7(^8S_{7/2}) \rightarrow 4f^65d$ transition [18,19]. The samples treated at 700 and 800 °C monitoring the emission at 615 nm (Fig. 4b) also display a broad band with maximum around 340 nm, corresponding to Eu^{2+} transition, and a group of sharp lines between 250 and 590 nm that are assigned to the intraconfigurational transitions from $^7F_0$ ground state to excited states of the Eu^{3+} ion [20–23]. However, the excitation spectra of sample heated at 900 °C monitoring the excitation at 615 nm of $^5D_0 \rightarrow {}^7F_2$ transition of Eu^{3+} ion exhibit a broad band assigned to the $O \rightarrow Eu^{3+}$ ligand-to-metal charge-transfer states (LMCT) around 280 nm (Fig. 4b).

The emission spectra of the samples treated at 700, 800 and 900 °C recorded in the spectral range from 450 to 750 nm, under excitation at 340 and 396 nm (at 77 K) are shown in Fig. 5a and b, respectively. The Fig. 5a shows a broadened band in the range of 450 to 550 nm assigned to the $4f^65d \rightarrow 4f^7$ ($^8S_{7/2}$) interconfigurational transition of Eu^{2+} ion [24,25] overlapped to the $^4F_{9/2} \rightarrow {}^6H_{15/2}$ intraconfigurational transition of the Dy^{3+} ion around 480 nm under excitation at 396 nm (insert Fig. 5a). Besides, the $^4F_{9/2} \rightarrow {}^6H_{13/2}$ transition (579 nm) of Dy^{3+} ion [26] is overlapped with the $^5D_0 \rightarrow {}^7F_0$ (578 nm) and $^5D_0 \rightarrow {}^7F_1$ (595 nm) transition from the Eu^{3+} ion. On the other hand, the hypersensitivity $^5D_0 \rightarrow {}^7F_2$ transition peak is the most intense one when recorded under excitation at 396 nm of Eu^{3+} ion (Fig. 6b). In these spectra, the

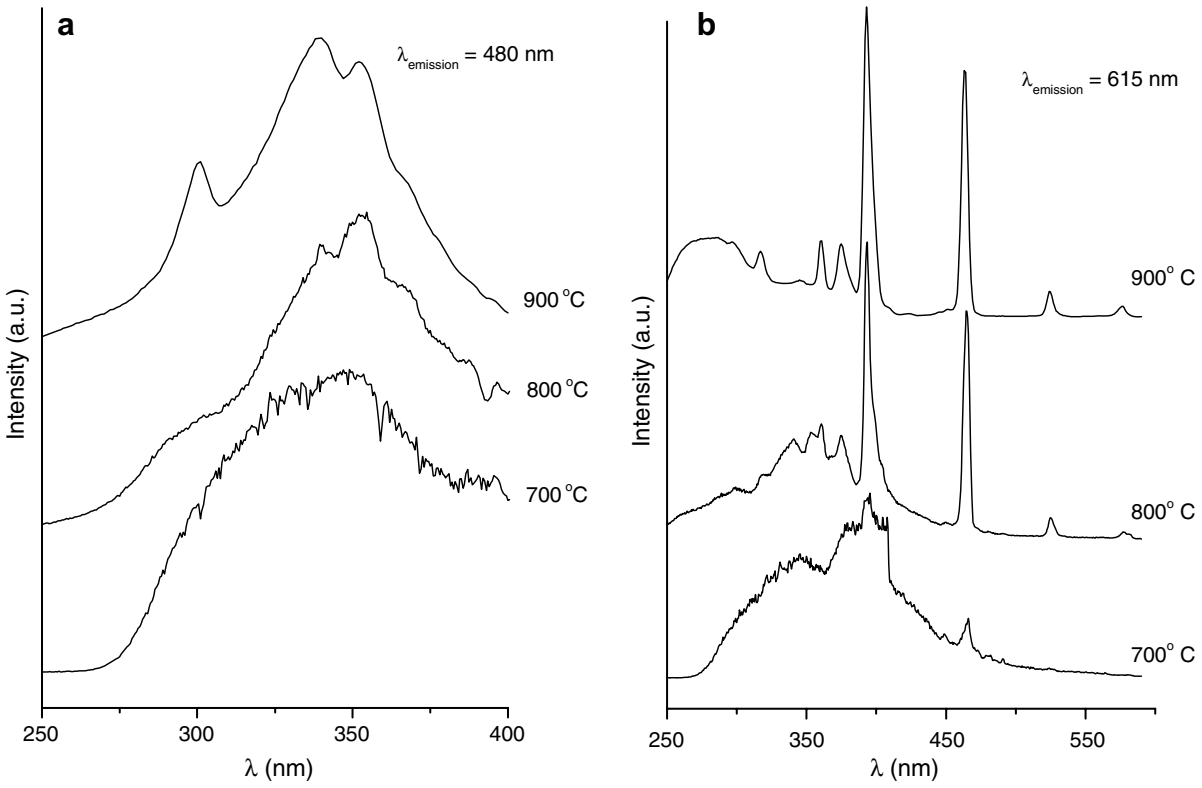

Fig. 4. Excitation spectra of $MgAl_2O_4$:Eu,Dy samples heated at 700, 800 and 900 °C monitoring the emission at 480 (a) and 615 nm (b).

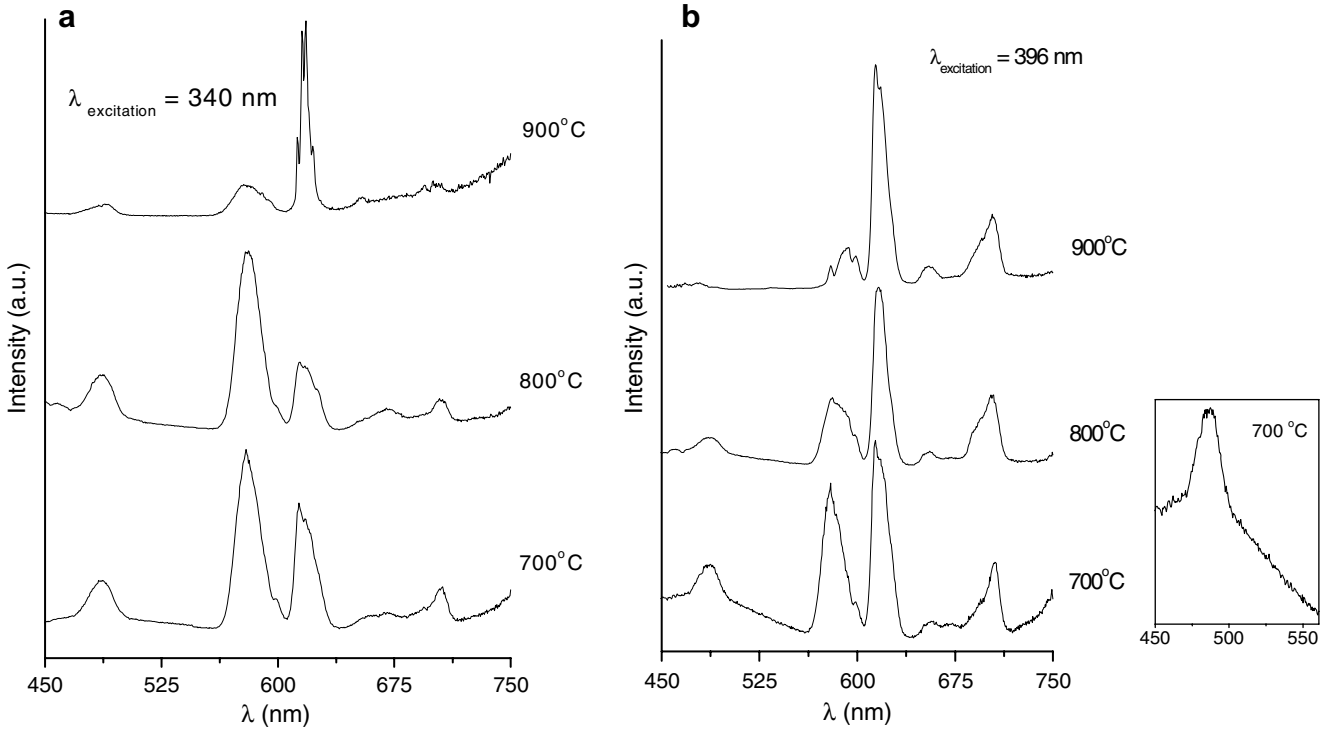

Fig. 5. Emission spectra of $MgAl_2O_4$:Eu,Dy samples heated at 700, 800 and 900 °C under excitation at 340 (a) and 396 nm (b).

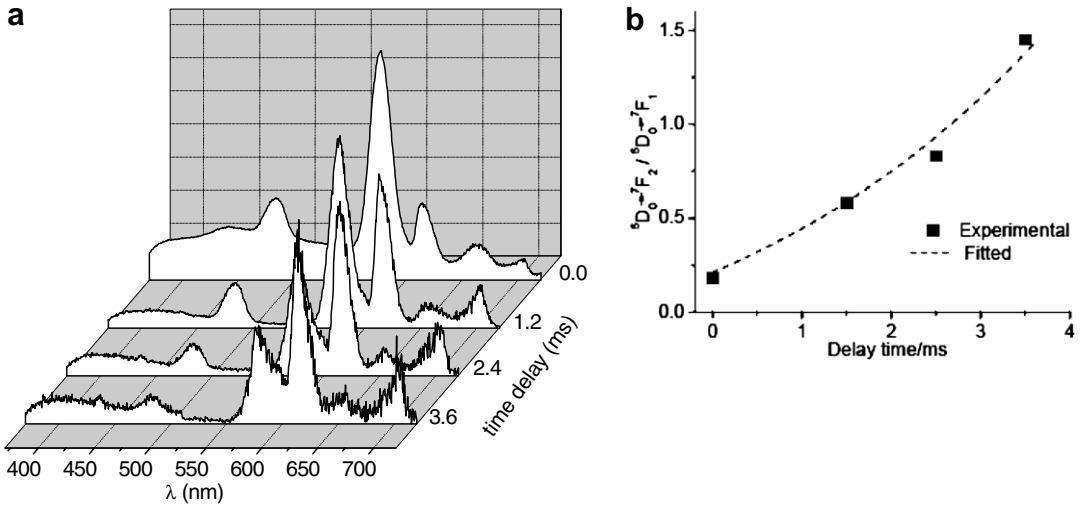

Fig. 6. (a) Time resolved luminescence spectra of $MgAl_2O_4$:Eu,Dy sample heated at 700 °C monitoring the excitation at 340 nm and (b) Curve of the η_{Eu} intensity parameter versus delay times (ms).

transitions $^5D_0 \rightarrow {}^7F_3$ and $^5D_0 \rightarrow {}^7F_4$ are observed around 665 and 710 nm, respectively. As it can be seen, the emission spectrum of the $MgAl_2O_4$:Eu,Dy phosphor annealed at 900 °C exhibits only the $^5D_0 \rightarrow {}^7F_0$, $^5D_0 \rightarrow {}^7F_1$, $^5D_0 \rightarrow {}^7F_2$ $^5D_0 \rightarrow {}^7F_3$ and $^5D_0 \rightarrow {}^7F_4$ transition arising from the trivalent europium ion, with the hypersensitivity $^5D_0 \rightarrow {}^7F_2$ transition dominant. It is observed that when this phosphor is prepared by citrate sol–gel method and thermally treated the Eu^{2+} ion oxidizes to the trivalent state with the increasing of the temperature (700, 800 and 900 °C). The presence of intense peak assigned to hypersensitive $^5D_0 \rightarrow {}^7F_2$ transition at 615 nm indicates that there is no inversion center around Eu^{3+} ion in sample heated at 900 °C.

The emission spectra of the phosphor materials recorded under excitation at 340 nm (Fig. 5b) show the same electronic transitions in the Fig. 5a. However, in the spectra of the compounds calcinated at 700 and 800 °C, the $^4F_{9/2} \rightarrow {}^6H_{13/2}$ transition (579 nm) of Dy^{3+} are more intense than the hypersensitivity $^5D_0 \rightarrow {}^7F_2$ transition of Eu^{3+} ion suggesting that the energy transfer for dysprosium is more efficient.

According to luminescence spectra, the reduction from trivalent europium to the divalent state is favored at 700–800 °C. The system heated at 900 °C contains a smaller amount of Eu^{2+} ion and the persistent luminescence is not as intense as the others observed with the material heated at lower temperatures.

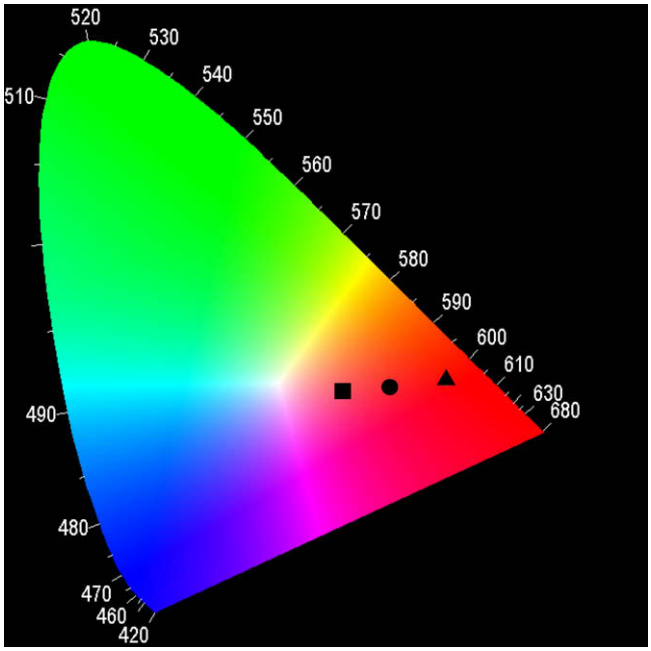

Fig. 7. Chromaticity coordinates from emission spectra of the samples under excitation at 396 nm, with ■ for 700 °C, ● for 800 °C and ▲ for 900 °C.

In Fig. 6a an increase of emission intensity of the $^5D_0 \rightarrow {}^7F_2$ hypersensitive transition with the increasing of delay time was observed. Time resolved spectra of sample heated at 700 °C (Fig. 6a) suggest the presence of multiple local symmetry sites around Eu^{3+} ion. One of sites presents the hypersensitive $^5D_0 \rightarrow {}^7F_2$ transition (forced electric dipole) as more prominent emission than $^5D_0 \rightarrow {}^7F_1$ transition. Since the intensity of the magnetic dipole transition $^5D_0 \rightarrow {}^7F_1$ is relatively insensitive to the chemical environment around of the Eu^{3+} ion, so that it may be used as the internal standard (reference transition).

Colour purity can be visualized in the chromaticity diagram (Fig. 7), as blue, red, and green vertex regions, with the emission colour coordinates of the luminescent material. The CIE (Comission Internacionale de l'Eclairage) chromaticity diagram of $MgAl_2O_4$:Eu,Dy samples at different temperatures were obtained using a Spectra Lux Software v.2.0 Beta [15]. For any given colour there is one setting for each three numbers X, Y and Z known as tristimulus values that will produce a match [27,28]. Based on emission spectra of $MgAl_2O_4$:Eu,Dy samples, the (x,y) colour coordinates were determined with the following values $(x,y) = (0.44, 0.32)$, $(0.51, 0.33)$ and $(0.59, 0.34)$ for the samples heated at different temperatures 700, 800 and 900 °C, respectively.

Fig. 7 shows that the colour shifts from bluish to reddish along with the variation of temperature from 700 to 900 °C. The sample at 700 °C exhibits non-monochromatic colour due to the presence of emission bands simultaneously arising from Eu^{2+} and Eu^{3+} ions [29].

4. Conclusion

The citrate sol–gel method is a good alternative route to the synthesis of $MgAl_2O_4$:Eu,Dy nanoparticles. XRD patterns indicated that the samples heated from 700 to 900 °C present almost complete crystallization in the $MgAl_2O_4$ spinel phase. By this method, Eu^{3+} ion is partially reduced to the divalent state during the calcination process due to the presence of carbonaceous material in the precursor. The solids heated at 700 and 800 °C present green persistent luminescence around 30 s after exposure to UV radiation. TEM images of $MgAl_2O_4$:Eu,Dy sample prepared at 800 revealed aggregates formed by sphere-like nanoparticles with grain sizes distributed around 20 nm.

The $MgAl_2O_4$:Eu,Dy phosphors show an emission band at 480 nm assigned to the $4f^65d \rightarrow 4f^7$ ($^8S_{7/2}$) transition of Eu^{2+} ion overlapped to the $^4F_{9/2} \rightarrow {}^6H_{15/2}$ transition of the Dy^{3+} ion. Besides, the $^4F_{9/2} \rightarrow {}^6H_{13/2}$ transition (579 nm) of Dy^{3+} ion is overlapped with the $^5D_0 \rightarrow {}^7F_{0-1}$ transitions from the Eu^{3+} ion. Excitation spectra of sample heated 900 °C with emission monitored at 615 nm of hypersensitive $^5D_0 \rightarrow {}^7F_2$ transition of Eu^{3+} ion exhibits the broaden band assigned to the $O \rightarrow Eu^{3+}$ ligand-to-metal charge-transfer states (LMCT) around 280 nm. It was observed that with an increasing of temperature, the colour shifts from bluish (700 °C) to reddish colour (900 °C), according to chromatic coordinates.

Acknowledgements

The authors thank Fundação de Amparo à Pesquisa do Estado de São Paulo (FAPESP), Conselho Nacional de Desenvolvimento Científico e Tecnológico (CNPq), Rede de Nanotecnologia Molecular e de Interfaces (RENAMI) and Instituto do Milênio de Materiais Complexos (IM^2C) for financial support. The authors also thank Prof. Dr. Sylvia Mendes Carneiro from Instituto Butantan for TEM image.

References

[1] T. Matsuzawa, Y. Aoki, N. Takeuchi, Y. Murayama, J. Electrochem. Soc. 143 (1996) 2670.
[2] J. Hölsa, T. Aitasalo, H. Junger, M. Lastusaari, J. Niittykoski, G. Spano, J. Alloys Compd. 374 (2004) 56.
[3] T. Aitasalo, P. Deren, J. Hölsa, H. Junger, J.-C. Krupa, M. Lastusaari, J. Legendziewicz, J. Niittykoski, W. Strek, J. Solid State Chem. 171 (2003) 114.
[4] T. Aitasalo, J. Holsa, H. Jungner, M. Lastusaari, J. Niittykoski, J. Phys. Chem. B 110 (2006) 4589.
[5] F. Pellé, T. Aitasalo, M. Lastusaari, J. Niittykoski, J. Hölsa, J. Lumin. 119–120 (2006) 64.
[6] D. Haranath, V. Shanker, H. Chander, P. Sharma, J. Phys. D Appl. Phys. 36 (2003) 2244.
[7] Y.H. Li, Z.L. Tang, Z.T. Zhang, C.W. Nan, Appl. Phys. Lett. 81 (2002) 996.
[8] J. Zhang, Z. Zhang, T. Wang, W. Hao, Mater. Lett. 57 (2003) 4315.
[9] S. Tanaka, I. Ozaki, T. Kunimoto, K. Ohmi, H. Kobayashi, J. Lumin. 87–89 (2000) 1250.
[10] G. Blasse, B.C. Grabmeier, Luminescent Materials, Springer Verlag, Berlin, 1994.
[11] T. Peng, L. Huajun, H. Yang, C. Yan, Mater. Chem. Phys. 85 (2004) 68.
[12] J. Sánchez-Benítez, A. de Andrés, M. Marchal, E. Cordoncillo, M.V. Regi, P. Escribano, J. Solid State Chem. 171 (2003) 273.
[13] Y. Liu, C.N. Xu, J. Phys. Chem. B 107 (2003) 3991.
[14] X.L. Jia, H.J. Zhang, Y.J. Yan, Z.J. Liu, Mater. Sci. Eng. A 379 (2004) 112.
[15] P.A. Santa-Cruz, F.S. Teles, Spectra Lux Software v.2.0 Beta, Ponto Quântico Nanodispositivos, RENAMI, 2003.
[16] B.D. Cullity, Elements of X-ray Diffraction, Addison-Wesley Publishing Company Inc., Reading, MA, 1967.
[17] K. Nakamoto, Infrared and Raman Spectra of Inorganic and Coordination Compounds, Willey-Interscience Publication, 1986.
[18] P. Dorenbos, J. Electrochem. Soc. 152 (2005) H107.
[19] P. Dorenbos, J. Lumin. 104 (2003) 239.
[20] J.G. Kang, M.K. Nah, S. Youngku, J. Phys-Condens. Mat. 12 (2000) L199.
[21] E.E.S. Teotônio, M.C.F. Felinto, H.F. Brito, O.L. Malta, A.C. Trindade, R. Najjar, W. Strek, Inorg. Chim. Acta 357 (2004) 451.
[22] R. Stefani, A.D. Maia, E.E.S. Teotonio, M.A.F. Monteiro, M.C.F.C. Felinto, H.F. Brito, J. Solid State Chem. 179 (2006) 1086.
[23] R. Stefani, A.S. Maia, E.E.S. Teotônio, C.A. Kodaira, M.C.F.C. Felinto, H.F. Brito, Opt. Mater. 29 (2007) 1852.
[24] F.C. Palilla, A. Levine, M. Tomkus, J. Electrochem. Soc. 115 (1968) 642.
[25] V. Singh, J.J. Zhu, M.K. Bhide, V. Natarajan, Opt. Mater. 30 (2007) 446.
[26] Z.F. Li, L. Zhou, J.B. Yu, H.J. Zhang, R.P. Deng, Z.P. Peng, Z.Y. Guo, J. Phys. Chem. C 111 (2007) 2295.
[27] K.M.N. Krishna Prasad, S. Raheem, P. Vijayalekshmi, C. Kamala Sastri, Talanta 43 (1996) 1187.
[28] CIE, Proceedings of 15th Session, Vienna, vol. A, 1963, p. 35 (p. 80 and 108).
[29] T. Justel, H. Nikol, C. Ronda, Angew. Chem. Int. Edit. 37 (1998) 3084.